Influence of Domain Orientation on the Mechanical Properties of Regenerated Cellulose Fibers

Kenny Kong,[†] Richard J. Davies,[‡] Michael A. McDonald,[§] Robert J. Young,[†] Michael A. Wilding,[||] Roger N. Ibbett,[||] and Stephen J. Eichhorn*,[†]

Materials Science Centre, School of Materials, University of Manchester, Grosvenor Street, Manchester M1 7HS, United Kingdom, European Synchrotron Radiation Facility, B.P. 220, F-38043 Grenoble Cedex, France, CCLRC Daresbury Laboratory, Warrington, Cheshire WA4 4AD, United Kingdom, and Textiles and Paper, School of Materials, University of Manchester, Sackville Street, Manchester, M60 4QD, United Kingdom

Received September 15, 2006; Revised Manuscript Received November 14, 2006

The determination of the crystal orientation of regenerated cellulose fibers produced under different drawing regimes is presented. Orientation is determined by using wide-angle X-ray diffraction from a synchrotron source and by measuring the azimuthal width of equatorial reflections. The orientation parameter $\langle \sin^2 \theta \rangle$ is then determined to compare fiber samples. By using a 500 nm beam size, clear differences between the crystal orientations of the skin and the core of the fibers are reported for a range of differently processed fibers for the first time. These results are shown to have implications for the mechanical properties of regenerated cellulose fibers. By applying tensile deformation to fiber bundles it is shown that the most misoriented samples undergo rapid decreases in the orientation parameter, which is an indication of crystal reorientation. However, the more highly oriented fibers undergo little reorientation. An average shear modulus for these fibers is determined by placing the data on a master curve and fitting with a model equation. By using another model for the fibers of low orientation and the shear modulus from the master curve analysis, it is shown that the deformation of less oriented fibers is dominated by shear between crystals, whereas the more oriented filaments are likely to undergo more significant chain deformation. By using a new model for fibers of low orientation, a parameter k_σ is introduced that gives the proportion of the fiber stress that is due to crystal shear. Systematic differences between this parameter for fibers of increasing initial orientation are reported. Moreover it is shown that the fibers of initially lower average orientation are governed by uniform strain, in agreement with the new model, whereas more highly oriented fibers deform under uniform stress. Furthermore, the model that we propose for misoriented domains and the use of a new factor dictating the proportion of shear stress may have general applications in materials engineering.

Introduction

Cellulose is a ubiquitous material and is found in higher plants, algae, bacteria, and some sea creatures such as tunicates.[1] When in the native state, cellulose chains, which are anhydroglucose units bonded to each other by β-1,4 glycosidic linkages, can develop a wide variety of architectures in the form of fibrils, which are sometimes helically wound within the cell walls of plant fibers.[2] However, when cellulose fibers are regenerated from the native state (cellulose I) into a more stable form (cellulose II) by a variety of processes, this architecture is predominantly lost. Nevertheless, the advantages of regeneration are numerous, such as the production of continuous fibers, reduction in the variability of mechanical properties, and control over the molecular orientation. It is this latter property that dominates the mechanics of drawn polymers in particular[3] and not just exclusively cellulose. Highly oriented cellulose fibers, produced from liquid crystalline precursors,[4,5] have high tensile strengths and Young's moduli[5,6] and therefore are used for a number of applications.

The commercial routes to cellulose regeneration are numerous, and some of them have been summarized by Woodings.[7] One of the most significant recent developments in this respect has been the ability to spin cellulose fibers from environmentally benign amine oxide solvents, such as in the "Lyocell" process.[7] It has long been known, since initial studies by Graenacher and Sallman,[8] that cellulose will readily dissolve in a nonderivative form in amine oxides. Structural studies of these fibers have been extensive (see refs 9−15 for some examples), but little has been reported on crystalline deformation. The molecular deformation of Lyocell fibers, using Raman spectroscopy, has been previously reported,[16−18] and some studies on the skin−core characteristics of pore geometries and orientations have been obtained using small-angle X-ray scattering (SAXS).[19] Recently, Gindl and co-workers have also shown that the skin−core orientations change in a bent lyocell fiber sample to higher and lower orientations on the tensile and compression sides of the filament, respectively.[20] They also obtained a uniform skin−core orientation for their fibers.[20] We show that the orientation distributions in fibers are not uniform, in contrast to Gindl et al.[20] This difference in results may be due to the fact that we use a submicron-sized beam whereas Gindl et al.[20] used a beam size of $5 \times 5\ \mu m^2$. We also show that samples with lower initial average orientation appear to reorient by a completely different mechanism, mainly reorientation and not chain deformation. The rate of crystal reorientation is proportional to the initial value

* Author to whom correspondence should be addressed. Phone: 0161 200 5982. Fax: 0161 200 3636. E-mail: S.J.Eichhorn@manchester.ac.uk.
[†] Materials Science Centre, University of Manchester.
[‡] European Synchrotron Radiation Facility.
[§] CCLRC Daresbury Laboratory.
[||] Textiles and Paper, University of Manchester.

10.1021/bm060877b CCC: $37.00
Published on Web 01/18/2007

of orientation for highly oriented fibers. These results have implications for the use of such fibers in technical applications, particularly in terms of mechanical properties.

Experimental Methods

Materials. The materials used in this study were experimentally spun cellulose fibers. All fibers were generated using a *N*-methlymorpholine *N*-oxide (NMMO) solvent with wood pulp as the source of the cellulose. The spinning "dope" contained 14% cellulose and 86% NMMO, and the fibers that are produced are in essence similar to that of a commercial lyocell fiber.

Fiber Spinning. Pilot-scale fiber spinning equipment (supplied by Tencel Ltd., which was owned then by Acordis Plc, and now by Lenzing AG) was used to produce fibers by wet-jet spinning. The spinning "dope" was placed into a heated spinneret (95 °C) and then extruded with controlled speeds through an air gap into a coagulation bath at a temperature of 25 °C. Water was used as a spinning bath to coagulate the dope. The dope was coagulated by exchanging NMMO and water, which is also thought to induce hydrogen bonding,[21] although the full hydrogen bond system only develops on drying. Continuous filaments of all fibers were wound onto a speed-controlled rotating drum and then washed with water and dried at room temperature. An important parameter called the draw ratio (D_R), which is the ratio of the winding speed to the dope extruding speed, is used to subsequently define each fiber. A number of draw ratios were investigated in this study, namely 8.9, 5.9, 3.0, 1.5, 1.1, and 0.7.

Skin−Core Orientation of Fibers Determined Using X-ray Diffraction. Microstructural characterization of the fibers was carried out at the European Synchrotron Radiation Facility (ESRF) on beamline ID13. The wavelength of the radiation used was 0.98 Å with a specimen to camera distance of approximately 95 mm. To determine the magnitude of the orientation parameter across each filament, the beamline was configured with the beam focused to a 500 nm spot size, and a MARCCD detector was used to collect wide-angle X-ray diffraction (WAXD) images. The WAXD patterns were obtained from the fiber width using a step size of 500 nm and an exposure time of 5 s. The orientation parameters across the fiber diameter were determined from the azimuthal widths of the equatorial peaks, an analysis that will be explained in more detail later.

To determine the magnitude of the orientation parameter $\langle \sin^2 \theta \rangle$ of the crystalline fraction, the intensity of the azimuthal spreading of the 200 equatorial reflection $\rho(\theta)$ was obtained by using the Fit2D software[22,23] and a caking integration. The 200 reflection was used as it is the most intense along the equator. Any fiber texture was not taken into consideration, and this remains a topic of further investigation. The conditions of this integration are shown in Figure 1, overlaid on a typical diffraction pattern. The intensity data were then fitted with a Lorentz IV function, using the Solver Excel function. This was done to reduce the influence of background noise in the diffraction patterns. The orientation parameter is defined by the equation[24]

$$\langle \sin^2 \theta \rangle = \frac{\int_0^{\pi/2} \rho(\theta) \sin^3 \theta \, d\theta}{\int_0^{\pi/2} \rho(\theta) \sin \theta \, d\theta} \quad (1)$$

where $\rho(\theta)$ is the distribution of the 200 reflection, measured directly from the azimuthal spreading of the equatorial reflections. For perfect crystallite orientation $\langle \sin^2 \theta \rangle = 0$, and hence, an increasing crystalline orientation gives rise to a decrease in the value of the orientation parameter.

Calculation of Average Orientation Parameter Weighted by Gauge Volume. The orientation parameters across the fiber diameter were determined by single fiber diffraction. However, it is necessary to weight the results taken across the fiber by gauge volume to determine the distribution and average value for a single fiber.

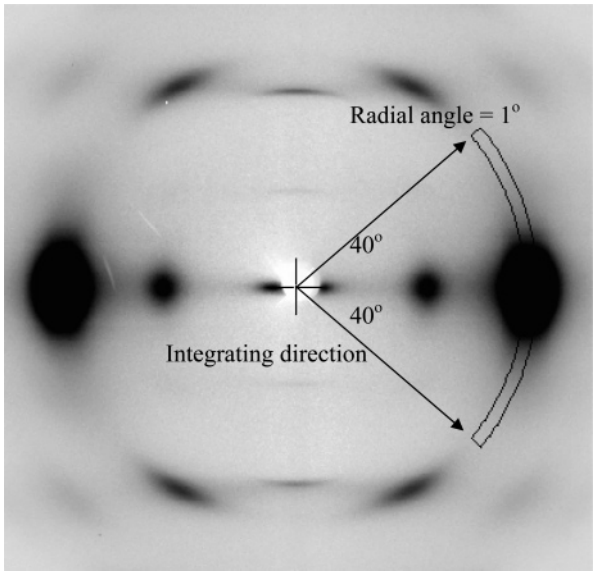

Figure 1. Conditions used for the caking integration to determine the azimuthal intensity distribution for the orientation parameter determination.

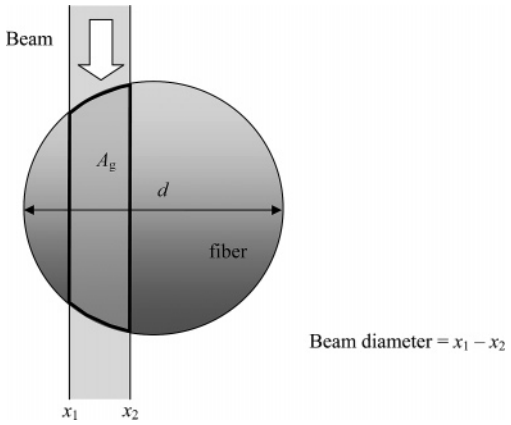

Figure 2. Schematic of the beam passing through a fiber gauge volume where d is the fiber diameter and A_g is a two-dimensional projection of gauge volume.

To calculate gauge volume weighted averages, it is necessary to determine the amount of material at each beam position across the fiber. Gauge volume is the amount of material through which the X-ray beam passes. By assuming that the fiber is cylindrical and that the beam spot size is constant across the fiber width, the calculation of gauge volume can be performed using the equation

$$A_g = 2 \int_{x_1}^{x_2} \sqrt{(d/2)^2 - x^2} \, dx \quad (2)$$

where

$$-d/2 < x_1 < x_2 < d/2$$

and A_g is the gauge volume, d is the fiber diameter, and x is the position of the fiber in the beam, as shown in Figure 2. Therefore, the weighted average is given by the equation

$$\langle \sin^2 \theta \rangle_{\text{average}} = \frac{\sum_n (\langle \sin^2 \theta \rangle_n A_{g,n})}{\sum_n A_{g,n}} \quad (3)$$

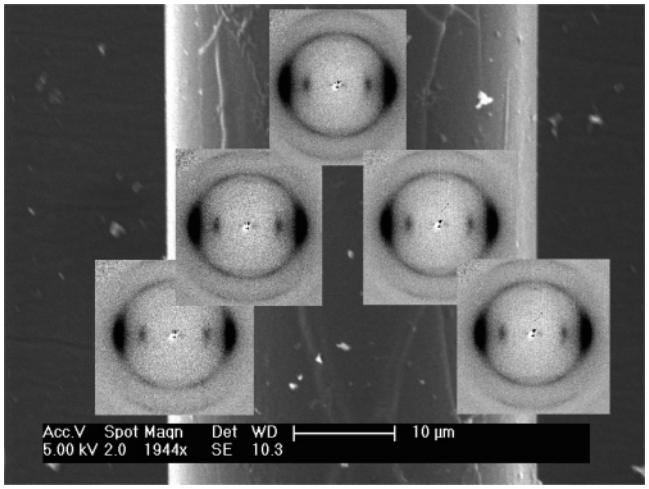

Figure 3. Diffraction patterns generated across a single fiber (D_R = 0.7) overlaid on a scanning electron micrograph.

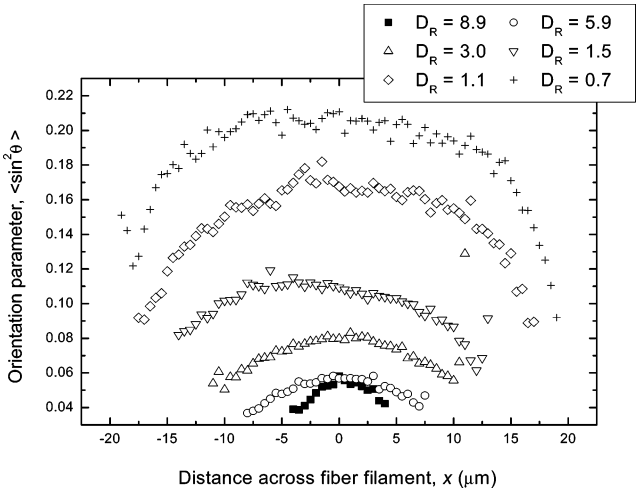

Figure 4. Orientation parameter distributions across fiber diameters for fibers produced with draw ratios of D_R = 8.9, 5.9, 3.0, 1.5, 1.1, and 0.7.

where $\langle \sin^2 \theta \rangle_{average}$ is the calculated average orientation parameter, $\langle \sin^2 \theta \rangle_n$ is the orientation parameter at the nth position on the fiber, and $A_{g,n}$ is the nth gauge area for that position.

Determination of Fiber Orientation during Deformation Using X-ray Diffraction. WAXD deformation studies of all samples were carried out on the protein crystallography beamline (station 14.1) at the Daresbury Synchrotron Radiation Source. The wavelength of the radiation used was 1.49 Å with a specimen to camera distance of approximately 70 mm. All samples were prepared as fiber bundles mounted onto 50 mm gauge length fiber cards, which were then screwed onto a customized straining rig with a 250 N load cell for determining fiber stress. Specimens were deformed in tension (in air) by the straining rig and were exposed to the X-ray beam for 30 s at each load level. Load was recorded using a transducer system, and the fiber stress was then calculated by subsequently counting the number of fibers in the bundles, multiplying by the cross-sectional area of one filament, and dividing the load by this value. The methods used to determine the cross-sectional area of these fibers have been reported previously.[17,18] It is worth mentioning that the beam size in this case was 30 μm in diameter and of low flux density, and hence it is not possible to obtain local orientation parameters but only an average. Fiber bundles were also necessary in this case due to the beam being larger than a fiber diameter.

Results and Discussion

Figure 3 reports generated WAXD patterns across a single fiber diameter, using a spot size of 500 nm. This is an ideal method for investigating so-called skin−core structural effects. A comparison for orientation parameter distributions of all samples is shown in Figure 4. First of all it is obvious that fibers produced using high draw ratios have smaller diameters than those produced at a lower draw ratio. The exact values of these diameters have been previously reported.[17]

It is clear that all fibers have a nonuniform skin to core crystal orientation, with a higher orientation within the skin of the fibers than the core. A similar phenomenon was observed in a previous study on viscose fibers[6] and can be explained in terms of the spinning process. When the spinning dope is passing through the spinneret, the shear forces on the outer region of the filament are higher, which, therefore, induces higher crystal orientation at the skin of the fiber. However, this clearly produces a hybrid structure in terms of orientation and highlights that bundle experiments really only yield average properties. Fibers spun with lower draw ratios, and therefore subsequently of lower average orientation, give rise to greater anisotropy between the skin and the core. This anisotropy is undesirable as it limits the mechanical properties of the resultant filament, in particular stiffness and strength. This will also have implications for the local deformation of fibers in terms of their reorientation, and this will now be discussed.

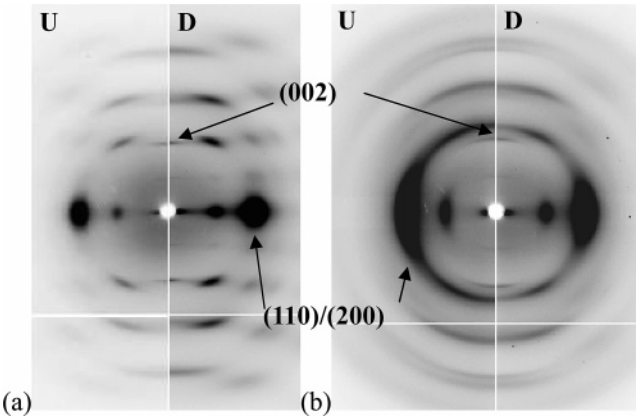

Figure 5. WAXD patterns of undeformed (U) and deformed (D) fiber bundle samples for (a) D_R = 8.9 and (b) D_R = 0.7. Stress levels are 0 GPa for undeformed and 0.11 and 0.19 GPa for the fibers with draw ratios of 8.9 and 0.7 respectively.

Typical WAXD patterns are shown in Figure 5 for undeformed and deformed fibers produced using two draw ratios (D_R = 8.9 and 0.7). It is clear that the sharpness of the equatorial reflections 110/200 for the sample produced using D_R = 8.9 is an indication of high orientation, which is in agreement with molecular orientation measurements using birefringence.[17] However, the equatorial reflections for the fiber produced using D_R = 0.7 are much broader, which is indicative of a much lower average orientation. The diffraction pattern of a deformed specimen of the highly oriented fiber (D_R = 8.9) has a similar diffraction pattern to the undeformed state, however with visibly much sharper reflections. This indicates that the highly oriented crystals reorient slightly toward the fiber axis upon the application of external tensile deformation, although there will be some consolidation and reorientation of fibers within the bundle that may give rise to increases in the sharpness of these reflections. Changes in crystallinity may also give rise to this, although we did not detect any significant increase in this parameter. Azimuthally integrated intensity plots of the 200 equatorial reflection for undeformed fibers of D_R = 8.9 and 0.7 are shown in Figures 6a and 6b. It can be seen that the width of these

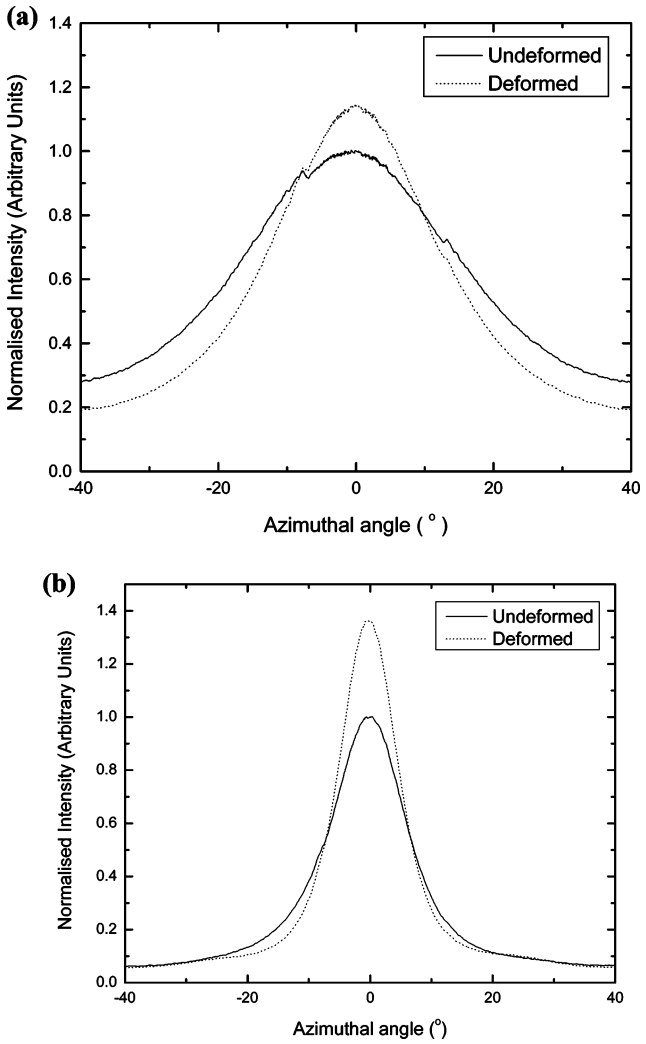

Figure 6. Intensity of the azimuthally integrated (200) reflection for (a) a fiber produced with $D_R = 0.7$ in an undeformed and deformed state and (b) for a fiber produced with $D_R = 8.9$ in an undeformed and deformed state. Stress levels are 0 GPa for the undeformed fibers and 0.11 and 0.19 GPa for the fibers with draw ratios of 8.9 and 0.7, respectively.

peaks differs depending on the draw ratio at which the fibers were produced, and this is used to determine the relative orientation parameters of each sample. The fiber produced with a low draw ratio ($D_R = 0.7$) has a much broader azimuthal intensity distribution than the fiber produced with a high draw ratio ($D_R = 8.9$). After deformation is applied, these azimuthal intensity distributions narrow for both fibers. The fiber produced with a low draw ratio shows the most dramatic change in the width of the azimuthal orientation distribution (Figure 6a) compared to the high draw ratio sample (Figure 6b), which is an indication that reorientation is more significant for the former. Discussions will now turn toward the analysis of the orientation parameter as a function of deformation for all fiber types.

Theoretical Approach to Fiber Micromechanics. For the fibers of lower orientation, it is thought that rotation dominates their behavior during tensile deformation and that the shear between crystals is high, as has been shown before using Raman spectroscopy (which follows molecular deformation).[18] Fiber mechanics, and in particular the Young's modulus of fibers, is affected by crystal orientation and also their reorientation during deformation. If the crystals are initially highly oriented, then one can expect that the fiber modulus will also be high. This is indeed the case for the fibers produced using a $D_R = 8.9$, which have previously been reported to have a Young's modulus of ~26 GPa, compared to ~11 GPa for fibers produced using $D_R = 0.7$.[17] However, the strain to failure of the fibers of lower orientation was found to be much greater than those with higher orientation. An analysis derived by Northolt et al.[24] has been used to relate the orientation parameter and shear modulus (g) by the relationship

$$\langle \sin^2 \Theta \rangle = \langle \sin^2 \Theta \rangle \exp(-2\sigma_c/g) \tag{4}$$

where $\langle \sin^2 \Theta \rangle$ is the initial second moment of the orientation parameter and σ_c is the crystal stress. The second moment of the orientation parameter ($\langle \sin^2 \Theta \rangle$) is not the same as the orientation parameter used in this study ($\langle \sin^2 \theta \rangle$). However, the latter can be approximated to within 10% of the second moment parameter below values of approximately 0.25.[25] This model has been confirmed for PpPTA fibers using an X-ray diffraction method.[24] If one assumes that the initial response of the deformation is elastic, not taking into account yielding, then

$$\sigma_c = \epsilon_c E_c \tag{5}$$

where E_c is the crystal modulus. One can therefore rewrite eq 4 with some manipulations as

$$\langle \sin^2 \theta \rangle = \exp(-2E_c\epsilon_c + \epsilon_o)/g \tag{6}$$

where

$$\epsilon_o = -g \ln(\langle \sin^2 \theta \rangle_0)/(2E_c) \tag{7}$$

and ϵ_c is crystal strain and ϵ_o is the strain required to change the orientation of any given fiber in the series to the value of the starting orientation of the next fiber. Crystals are assumed to rotate due to shear forces between them according to the schematic shown in Figure 7. It can be seen from the model that the effects of crystal strain and orientation parameter depend on the value of ϵ_o, which is determined by the initial orientation parameter and associated to the starting point along the first-order exponential decay curve. Therefore all experimental data lie a along a master curve (eq 6) with their positions according to their initial orientation parameter as

$$\langle \sin^2 \theta \rangle = \exp(-2E_c\epsilon_c/g) \tag{8}$$

Equation 8 was fitted to the experimental data, the result of which is shown in Figure 8. To obtain the crystal strain we used the change in the position of the 002 meridional reflections with respect to the center of the diffraction pattern, as has been done previously for a number of cellulose fibers.[6,26] The orientation parameter decreases as tensile deformation proceeds, as shown in Figure 8, which indicates that the average crystalline orientation is increasing in the fibers. It can be clearly seen that the samples have different starting orientation parameters, depending on the draw ratio used in production, indicating that the crystal orientation depends on the value of stress applied to the fiber during processing. Upon tensile deformation, the lowest draw ratio fiber ($D_R = 0.7$) shows the highest rate of reorientation, and this rate decreases with increasing draw ratio.

Figure 8 shows that eq 8 correlates well with the data, and a value of 1.96 GPa for the shear modulus is obtained using a value of 98 GPa for the crystal modulus from a theoretical

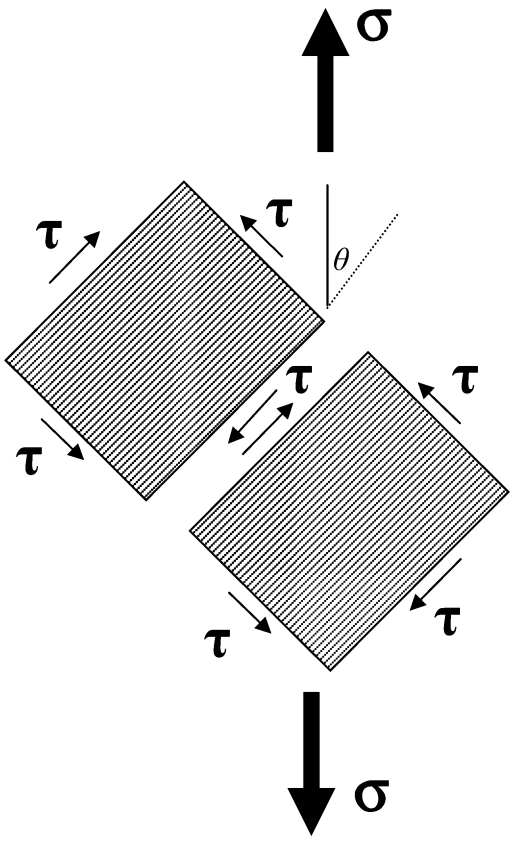

Figure 7. Schematic of the deformation of adjacent misoriented crystalline domains where σ are the applied stresses and τ are the shear forces.

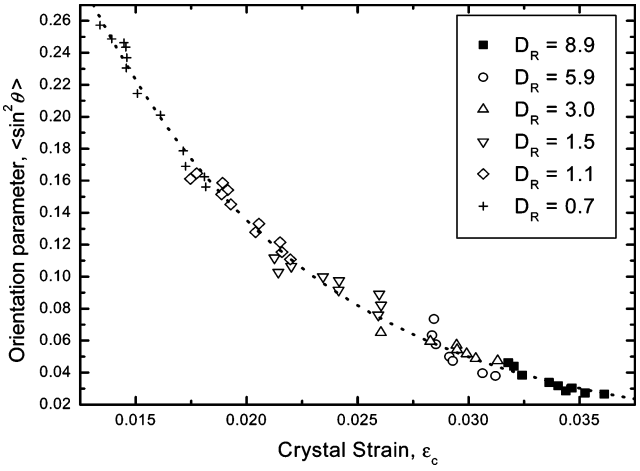

Figure 8. Changes in the orientation parameter as a function of the crystal strain showing a fit (dotted line) to the data using eq 4. (The χ^2 value of the fit was 3.7×10^{-5}.)

prediction.[26] This suggests that the mechanics of the crystal orientation are constrained by the crystal modulus and the shear modulus. According to eq 8, since the orientation parameter and crystal strain are closely related, it is impossible to observe either crystal straining or reorientation as separate entities. The value of the shear modulus obtained using this method is, however, at the lower end of the range of some values obtained by Northolt and deVries[27] and Eichhorn et al.,[6] which were between 1.8 and 3.8 GPa for some other types of regenerated cellulose fibers.

Figure 9a shows orientation data more linearly related to the bundle stress for the fibers produced with the range of D_R =

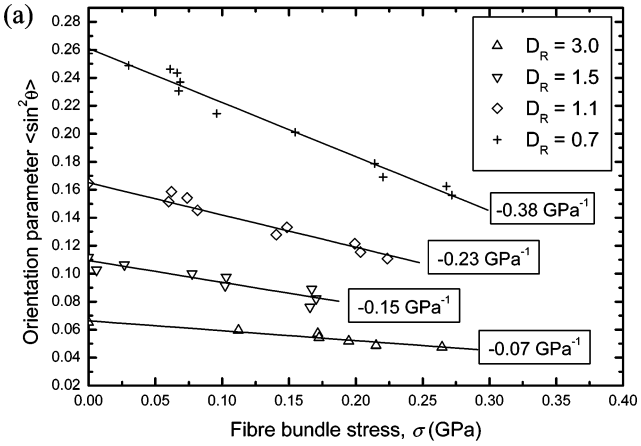

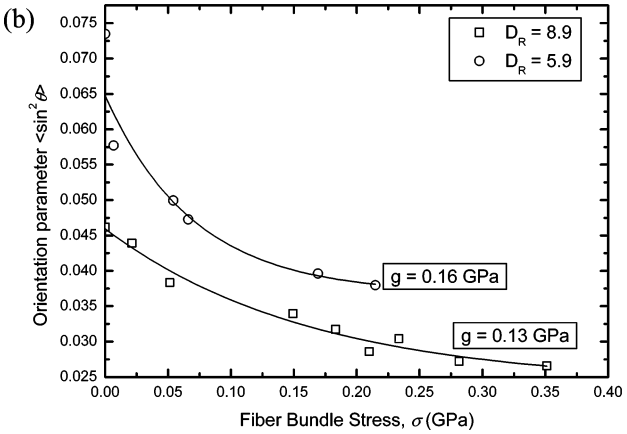

Figure 9. Change in orientation parameter $\langle \sin^2 \theta \rangle$ as a function of fiber bundle stress for (a) samples spun with draw ratios of 3.0, 1.5, 1.1, and 0.7 (solid lines are eq 13 and the figures are the gradients of the linear fits to the data) and (b) samples spun with draw ratios of 8.9 and 5.9 (solid lines are eq 4 with the calculated shear modulus (g) quoted). All correlation coefficients (R^2) for the fits to the data are greater than 0.9.

0.7−3.0 compared to those produced using a high draw ratio (D_R = 8.9 and 5.9, Figure 9b). If one assumes that reorientation of crystals in the fibers is the dominant behavior, and hence we can distinguish the two phenomena for the lower oriented material, and that crystals reorient under shear (as in Figure 7), then we can say that

$$\frac{\langle \sin^2 \theta \rangle - \langle \sin^2 \theta \rangle_0}{\langle \sin^2 \theta \rangle_0} = \gamma_c \qquad (9)$$

where $\langle \sin^2 \theta \rangle_0$ is the initial orientation parameter and γ_c is the crystal shear strain. It is assumed that elastic behavior of the material occurs and that there is negligible extension of the chains (i.e., predominantly orientation of the crystals dictates the mechanics of the fibers). We also have to assume that the structure responds under uniform strain; i.e., the shear strain is equal to the strain in the crystalline and amorphous regions. One cannot also distinguish between shear within crystals and shear between crystals. We assume however that the crystals themselves do not shear significantly and that the dominant shear forces are between crystals.

It is true that even in the lesser oriented fibers some domains will be oriented toward the fiber axis and hence will undergo significant chain extension. We merely argue that the dominant

Table 1. Values of the k_σ Parameter from Fits of Eq 13 to the Reorientation Data for Fibers with a Range of Draw Ratios D_R = 0.7−3.0

draw ratio	k_σ
0.7	0.74
1.1	0.45
1.5	0.31
3.0	0.14

behavior is dictated by the misoriented domains. Rearrangement of eq 9 leads to the relationship

$$\langle \sin^2 \theta \rangle = \gamma_c \langle \sin^2 \theta \rangle_0 + \langle \sin^2 \theta \rangle_0 \quad (10)$$

If we say that the crystal shear strain is governed by the equation

$$\gamma_c = \frac{\tau}{g} \quad (11)$$

where τ is the shear stress on a crystal (as schematically shown in Figure 7) and g is the shear modulus and that the shear stress will be scaled with the applied fiber bundle stress (σ) as

$$\tau = k_\sigma \sigma \quad (12)$$

where k_σ is a constant (or scaling factor) (k_σ may in reality be a function of $\langle \sin^2 \theta \rangle$, but for now we will for simplicity keep it constant), then we can write eq 10 as

$$\langle \sin^2 \theta \rangle = \frac{k_\sigma \sigma}{g} \langle \sin^2 \theta \rangle_0 + \langle \sin^2 \theta \rangle_0 \quad (13)$$

Equation 13 indicates that there ought to be a linear relationship between the orientation parameter and the stress, which agrees well with the data shown in Figure 9a for the fibers with the lower orientations. If one determines the k_σ parameter for each fiber from the slopes of the linear fits to the data shown in Figure 9a, then one obtains the values reported in Table 1. As one can see these values of the k_σ parameter decrease for increasing draw ratios, which suggests that as the crystals become more oriented the shear stresses between crystals get lower. Therefore this k_σ parameter is useful for determining, from eq 7, the relative contribution of shear between crystals for misoriented fibers.

When the fibers are highly oriented (for D_R = 8.9 and 5.9), the reorientation of domains with fiber bundle stress can be modeled using eq 4 and shear moduli calculated as shown in Figure 9b. These moduli are quite low compared to the average value determined from the master curve analysis. It is difficult to say with any confidence which are the correct values, given that no independent values of this parameter have been obtained. Measurements of the shear modulus of single crystals are perceivably difficult to perform but remain a topic for future investigation.

Given that the skin and the core orientations are clearly different, which is only perceptible when using the submicron beam, it might be the case that when the fibers are deformed that the less oriented domains in the bulk predominantly undergo orientation changes, whereas the skin might be expected to exhibit domain stretching. We have no evidence for this, as deformation was not applied using the submicron beam. Our models are also applied to composite orientation parameters for the bundle specimens, and it would be useful to apply these techniques to our single fiber samples. However, this type of experiment has been reported previously for PBO fibers, where it was shown that the orientation distribution from skin to core of the fibers became more uniform after applied tensile deformation.[28] This however occurred with no appreciable differences in skin and core crystal strains,[28] but for cellulose fibers this would require confirmation.

Conclusions

It has been shown that X-ray diffraction can be used to both determine the orientation and rate of reorientation of regenerated cellulose fibers. Regenerated cellulose fibers produced using high draw ratios have on average higher crystal orientation than those produced using lower draw ratios. The skin−core orientation of the fibers has been shown to be nonuniform, with the skin of the fibers having higher average orientation than the core. This has implications for the mechanical properties of these fibers, as a more uniform skin−core orientation may permit higher moduli, and this could be a topic for further investigation. This skin−core difference is thought to be due to the higher shear forces generated at the spinneret at these higher draw ratios. Fibers produced using a high draw ratio have been shown to reorient in a completely different way to those produced using a low draw ratio. All data can be fitted using a master curve if one assumes that the crystal and shear moduli are the same for all fibers. However, by splitting the two fiber types (oriented and less oriented), models based on uniform stress and uniform strain have been shown to fit data from these samples, respectively. A new model parameter has been introduced that gives the proportion of the fiber stress due to shear for the least oriented sample. This is shown to systematically change with both draw ratio, and therefore initial orientation, and perhaps is more appropriate for these types of cellulose fibers. Furthermore, the model that we propose for misoriented domains and the use of a new factor dictating the proportion of shear stress may have general applications in materials engineering. The shear modulus obtained by fitting a uniform stress model to the highly oriented fibers is lower than that determined previously by other methods and remains a topic for further investigation.

Acknowledgment. The authors thank the Engineering and Physical Sciences Research Council for funding the Ph.D. studentship under Grant No. GR/S44471. The authors also acknowledge the CCLRC and the ESRF for the allocation of beamtime at their respective synchrotrons. Lenzing are also acknowledged for the use of their pilot-scale spinning apparatus. Mr. Marek Hejda and Dr. Jim Bennett are also acknowledged for their assistance during the synchrotron experiments.

References and Notes

(1) Klemm, D.; Phillip, B.; Heinze, T.; Heinze, U.; Wagenknecht, W. *Comprehensive Cellulose Chemistry: Fundamentals and Analytical Methods*, Wiley-VCH: Weinheim, Germany, 1998; Vol. 1.
(2) Morton, W. E.; Hearle, J. W. S. *Physical Properties of Textile Fibres*; Textile Institute: Manchester, U. K., 1993.
(3) Ward, I. M. *Proc. Phys. Soc., London* **1962**, *80*, 1176.
(4) Boerstoel, H.; Maatman, H.; Westerink, J. B.; Koenders, B. M. *Polymer* **2001**, *42*, 7371.
(5) Northolt, M. G.; Boerstoel, H.; Maatman, H.; Huisman, R.; Veurink, J.; Elzerman, H. *Polymer* **2001**, *42*, 8249.
(6) Eichhorn, S. J.; Young, R. J.; Davies, R. J.; Riekel, C. *Polymer* **2003**, *44*, 5901.
(7) Woodings, C. R. *Int. J. Biol. Macromol.* **1995**, *17*, 305.
(8) Graenacher, C.; Sallmann, R. U. S. Patent 2,179,181, 1939.
(9) Lenz, J.; Schurz, J.; Wrentschur, E. *Holzforschung* **1988**, *42*, 117.
(10) Lenz, J.; Schurz, J.; Wrentschur, E. *J. Appl. Polym. Sci.* **1988**, *35*, 1987.
(11) Lenz, J.; Schurz, J. *Cellul. Chem. Technol.* **1990**, *24*, 3.
(12) Lenz, J.; Schurz, J. *Cellul. Chem. Technol.* **1990**, *24*, 679.
(13) Lenz, J.; Schurz, J.; Wrentschur, E. *Acta Polym.* **1992**, *43*, 307.

(14) Lenz, J.; Schurz, J.; Wrentschur, E. *Colloid Polym. Sci.* **1992**, *271*, 460.
(15) Schurz, J.; Lenz, J. *Macromol. Symp.* **1994**, *83*, 273.
(16) Hamad, W. J.; Eichhorn, S. J. *J. Eng. Mater. Technol.* **1997**, *119*, 309.
(17) Kong, K.; Eichhorn, S. J. *Polymer* **2005**, *46*, 6380.
(18) Kong, K.; Eichhorn, S. J. *J. Macromol. Sci., Phys.* **2005**, *44*, 1123.
(19) Moss, C. E.; Butler, M. F.; Muller, M.; Cameron, R. E. *J. Appl. Polym. Sci.* **2001**, *83*, 2799.
(20) Gindl, W.; Martinschitz, K. J.; Boesecke, P.; Keckes, J. *Cellulose* **2006**, *13*, 621.
(21) Chanzy, H.; Nawrot, S.; Peguy, A.; Smith, P.; Chevalier, J. *J. Polym. Sci., Polym. Phys. Ed.* **1982**, *20*, 1909.
(22) Hammersley, A. P. *Fit2D: An Introduction and Overview*; ESRF Internal Report ESRF97HA02T; 1997.
(23) Hammersley, A. P.; Riekel, C. *Synchrotron Radiat. News* **1989**, *2*, 24.
(24) Northolt, M. G. *Polymer* **1980**, *21*, 1199.
(25) Baltussen, J. J. M. Tensile Deformation of Polymer Fibers. Ph.D. Thesis, Technical University of Delft, Delft, The Netherlands, 1996.
(26) Eichhorn, S. J.; Young, R. J.; Davies, G. R. *Biomacromolecules* **2005**, *6*, 507.
(27) Northolt, M. G.; de Vries, H. *Angew. Makromol. Chem.* **1985**, *133*, 183.
(28) Davies, R. J.; Montes-Moran, M. A.; Riekel, C.; Young, R. J. *J. Mater. Sci.* **2003**, *38*, 2105.

BM060877B